EARTH SURFACE PROCESSES AND LANDFORMS
Earth Surf. Process. Landforms (2019)

Published online in Wiley Online Library
(wileyonlinelibrary.com) DOI: 10.1002/esp.4550

Sedimentary processes at ice sheet grounding-zone wedges revealed by outcrops, Washington State (USA)

Brian P. Demet,*† Jeffrey A. Nittrouer, John B. Anderson and Lauren M. Simkins‡
Department of Earth, Environmental and Planetary Sciences, Rice University, 6100 Main Street, Houston, Texas USA

Received 26 May 2017; Revised 10 November 2018; Accepted 12 November 2018

*Correspondence to: B. P. Demet, Rice University, Department of Earth, Environmental and Planetary Sciences, 6100 Main Street, Houston, Texas USA.
E-mail: demet010@umn.edu
†Current Affiliation: Schuepbach Energy Exploration, 2651 North Harwood, Suite 570, Dallas, Texas USA

‡Now at University of Virginia, Clark Hall 205, 291 McCormick Road, Charlottesville, Virginia, USA

ESPL
Earth Surface Processes and Landforms

ABSTRACT: Grounding-zone wedges (GZWs) mark the grounding terminus of flowing marine-based ice streams and, in the presence of an ice shelf, the transition from grounded ice to floating ice. The morphology and stratigraphy of GZWs is predominantly constrained by seafloor bathymetry, seismic data, and sediment cores from deglaciated continental shelves; however, due to minimal constraints on GZW sedimentation processes, there remains a general lack of knowledge concerning the production of these landforms. Herein, outcrop observations are provided of GZWs from Whidbey Island in the Puget Lowlands (Washington State, USA). These features are characterized by prograded diamictons bounded by glacial unconformities, whereby the lower unconformity indicates glacial advance of the southern Cordilleran Ice Sheet and the upper unconformity indicates locally restricted ice advance during GZW growth; the consistent presence of an upper unconformity supports the hypothesis that GZWs facilitate ice advance during landform construction. Based on outcrop stratigraphy, GZW construction is dominated by sediment transport of deformation till and melt-out of entrained basal debris at the grounding line. This material may be subsequently remobilized by debris flows. Additionally, there is evidence for subglacial meltwater discharge at the grounding line, as well as rhythmically bedded silt and sand, indicating possible tidal pumping at the grounding line. A series of GZWs on Whidbey Island provides evidence of punctuated ice sheet movement during retreat, rather than a rapid ice sheet lift-off. The distance between adjacent GZWs of 10^2–10^3 m and the consistency in their size relative to modern ice stream grounding lines suggests that individual wedges formed over decades to centuries.

KEYWORDS: grounding zone wedge; Puget lowlands; outcrop; stratigraphy; meltwater; ice sheet

Introduction

Geological records of paleo-ice sheets constrain spatiotemporal patterns of ice retreat and advance, and such information is necessary to evaluate ice mass changes and the contribution of ice sheets to sea-level changes over time scales of decades to millennia (DeConto and Pollard, 2016; Shepherd and Wingham, 2007; Rignot and Jacobs, 2002; Pritchard *et al.,* 2009). Furthermore, ice sheet reconstructions are necessary to validate the hindcasting capability of numerical models that are used to project future ice sheet mass balance associated with global climate change (Golledge *et al.,* 2015; DeConto and Pollard, 2016). Grounding line landforms, such as recessional moraines and grounding zone wedges (GZWs), form at the location where flowing ice ceases to be in contact with the bed (Powell, 1991; Powell and Domack, 1995; Powell and Alley, 1997; Alley *et al.,* 2007). As such, sedimentary deposits that build these landforms mark former grounding line positions of retreating marine-terminating glaciers and ice sheets. Generally, GZWs differ from moraines in their asymmetric wedge shape and exclusivity to subaqueous glacial environments. Typically, these landforms are found in glacial troughs and fjords occupied by fast-flowing ice streams and outlet glaciers (Batchelor and Dowdeswell, 2015; Simkins *et al.,* 2018).

Observations of GZWs on deglaciated continental margins usually rely upon marine geophysical methods, such as multibeam bathymetry and other lower frequency seismic data, which depict the planform geometry and image the interior stratigraphy of these deposits (Shipp *et al.,* 1999; Winsborrow *et al.,* 2010; Bart and Cone, 2012; Dowdeswell and Fugelli, 2012; Batchelor and Dowdeswell., 2015; Anderson and Jakobsson, 2017; Bart *et al.,* 2017). As has been documented in many studies, the deposit morphology is asymmetric, overlying a glacial unconformity formed by previous ice advance over the seafloor. The internal structure, based on seismic observations, includes foreset beds that downlap onto a basal unconformity, indicating progradation in the direction of net ice

flow (Figure 1). GZWs may also be characterized by chaotic acoustic patterns, which are interpreted to indicate reworking and deformation of foresets after initial sediment deposition (Shipp *et al.,* 1999; Howat and Domack, 2003; Dowdeswell and Fugelli, 2012). Variability in GZW morphology, such as size, shape, and sinuosity, primarily reflects differences in the duration of landform growth and spatiotemporal variability in grounding line sediment accumulation (Simkins *et al.,* 2018).

Sedimentological characterization of GZWs has been restricted to continental shelf sediment cores and high-resolution seismic profiles. An abundance of GZW research from the Ross Sea (Antarctica) provides a framework whereby sediment deposition patterns are used to infer ice dynamics and transport processes. For example, Howat and Domack (2003) describe six acoustic facies within GZWs of the western Ross Sea, which they argue represent a complete series grounding line retreat. Bart and Cone (2012) and Bart and Owolana (2012) examined cores recovered from topset, foreset and bottomset strata of a large composite GZW of the central Ross Sea continental shelf. Foraminiferal analyses revealed both reworked and *in situ* foraminiferal assemblages, indicating that the diamictons include both proximal glacimarine sediments and debris flows. Detailed sediment facies analysis of similar strategically placed cores from a large composite GZW in Whales Deep Basin on the outer continental shelf of the eastern Ross Sea revealed a stratigraphic succession consisting of diamictons overlain by proximal glacimarine sediments, including a sub-ice shelf facies, and capped by open marine sediments (McGlannan *et al.,* 2017). An abundance of reworked diatoms within diamictons was interpreted as indicating a combination of glacial and sediment gravity flow processes acting near the grounding line.

Prothro *et al.* (2017) provide detailed sediment facies analyses of cores from grounding zone wedges in the western Ross Sea, noting that glacimarine diamictons vary in thickness and are restricted to within 1.2 km of the grounding line. Grounding line-proximal sediments grade sharply into muds with little ice-rafted material; these deposits are interpreted as meltwater plume deposits.

Although GZW morphology, internal stratigraphy, and sediment source have been evaluated in prior research (Ottesen *et al.,* 2008; Li *et al.,* 2011; Dowdeswell and Fugelli, 2012), there nevertheless remains limited information regarding sedimentary processes that build GZWs and thereby affect planform patterns as well as internal sedimentary architecture. For example, sediment fluxes at the grounding line, and sediment transport styles along foreset beds, remain largely unconstrained due to limited measurements. Remote observations indicate that sediment flux to the grounding line is dominated by delivery of deformation till, meltout of basal material entrained within the ice, and sediment-laden meltwater discharge (Alley *et al.,* 1987; Christoffersen *et al.,* 2010). The flux of entrained basal sediment scales with ice velocity and debris concentration, and is postulated to provide at least an equivalent, if not possibly greater sediment flux relative to the discharge of deformation till (Christoffersen *et al.,* 2010). Upon depositing at the grounding line, sediment is subjected to remobilization by sediment failures, gravity flows, and reworking by meltwater discharge (King *et al.,* 1991; Powell and Alley, 1997; Horgan *et al.,* 2013). Ultimately, sediment flux and transport mechanisms along a grounding line vary in time and space, attributable, at least partially, to variable subglacial hydrology (Christoffersen *et al.,* 2010; Simkins *et al.,* 2018). Limited estimates of sediment flux have been reported, with values ranging from 40 m^3 a^{-1} near the modern Whillans Ice Stream grounding line (Hodson *et al.,* 2016) to 8000 m^3 a^{-1} for the paleo-Norwegian Channel Ice Stream (Nygård *et al.,* 2007).

GZWs are believed to play an important role in stabilizing ice sheets. For example, radar surveys across the modern grounding line of the Whillans Ice Stream (Siple Coast, West Antarctic Ice Sheet) suggest the presence of an actively forming GZW (Anandakrishnan *et al.,* 2007) that could provide stability to the ice sheet margin by building relief at the grounding line and thus elevating ice above its buoyancy threshold (Alley *et al.,* 2007), thereby potentially buffering ice-sheet instabilities caused by atmospheric and oceanic warming. Indeed, seismic surveys indicate erosional truncation of GZW topsets (Anderson, 1999) and the presence of subglacial lineations extending to the topset–foreset break (Mosola and Anderson, 2006; Bart and Cone, 2012; Jakobsson *et al.,* 2012; McMullen *et al.,* 2016; Bart *et al.,* 2017) that, in addition to foreset progradation, indicate local ice advance during GZW development.

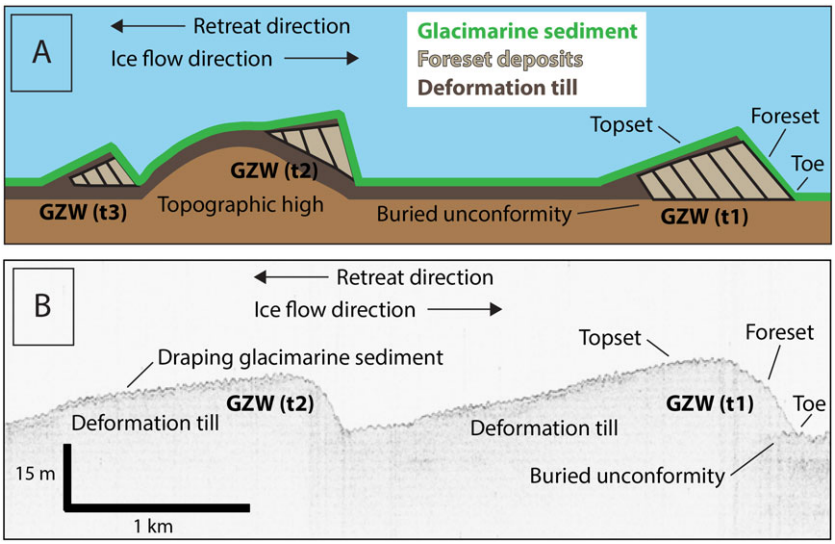

Figure 1. (A) simplified facies model based on observations from seismic data of the internal structure of GZWs from a deglaciated continental shelf, showing three GZWs that indicate punctuated grounding line retreat at time 1 (t1) to time 3 (t3). (B) High-frequency (3.5 kHz) seismic data across two backstepping intermediate-scale GZWs in Pennell Trough, western Ross Sea Antarctica, where the GZWs prograde over a buried unconformity but the internal structure is not resolved. [Colour figure can be viewed at wileyonlinelibrary.com]

To assess the mechanisms and time scales of GZW formation, as well as the role GZWs have in stabilizing grounding line positions, it is necessary to investigate the sedimentary processes forming GZWs. Herein, prograded diamictons located on Whidbey Island (Washington State, USA) generate landform outcrops that are interpreted as GZWs, based on criteria consistent with previous observations of GZWs on deglaciated continental shelves. These outcrops provide an opportunity for detailed analysis of the sedimentary deposits, which may be used to infer processes involved in GZW formation.

Whidbey Island Glacial History Since the Last Glacial Maximum

During and following the LGM, and specifically during the Fraser Glaciation (19 500–15 500 cal. Yrs B.P.; Easterbrook, 1963; Armstrong *et al.,* 1965), the Puget Lowlands were a shallow marine environment occupied by the Puget and Juan de Fuca lobes of the Cordilleran Ice Sheet (Figure 2(A)). As ice retreated, the region experienced isostatic uplift of 45 to 140 m (Thorson, 1989), exposing numerous submarine glacial landforms as outcrops that comprise the present-day sea cliffs of the region (Easterbrook, 1963, 1986; Armstrong *et al.,* 1965; Domack, 1983; Clague and James, 2002; Simkins *et al.,* 2017a). Sedimentary deposits of the Fraser advance and retreat include Vashon Till, conformably overlain by the glacimarine Everson Drift that records the deglacial history of the southern Cordilleran Ice Sheet (Easterbrook, 1963, 1986, 1994; Armstrong *et al.,* 1965; Swanson and Caffee, 2001). Radiocarbon ages from shells within the Everson Drift cluster around 15 500 cal. Yrs B.P. (Porter and Swanson, 1998; Swanson and Caffee, 2001; Booth *et al.,* 2003) (Figure 2(B)). This indicates the establishment of open marine conditions at this time, which has been interpreted to indicate rapid (geologically instantaneous) retreat of the southern Cordilleran Ice Sheet due to marine incursion through the Strait of Juan de Fuca (Easterbrook, 1994, 2003; Booth *et al.,* 2003). This interpretation, however, is based on ages obtained from shells that post-date retreat of the southern Cordilleran Ice Sheet, therefore dating the occurrence of marine conditions, rather than past Cordilleran Ice Sheet positioning. The chronological spread (Figure 2(B)) and lack of age control for the GZW deposits leave uncertainty with regard to the ice retreat timing and style.

Methods

Field outcrop study sites were focused on exposures of Vashon Stade strata of the Fraser Glaciation on Whidbey Island, Washington (Figure 2(A)). Publicly available satellite and topographic imagery from Google were used to identify outcrops located on the coastline that contained diamictons and low-angle foreset bedding stratigraphy. A LIDAR dataset with a 6 ft (1.8 m) spatial resolution from the Puget Sound LIDAR Consortium was used to characterize surface topography and determine surface slope changes (Figure 3). Field work included measuring stratigraphic sections, evaluating sedimentary structures, and producing lithological descriptions of exposed glacial and glacimarine deposits at three locations, referred to as Fort Casey (FC), Driftwood (DW) and West Beach (WB) (Table I). Facies are labelled by location abbreviation from the stratigraphically lowest to uppermost units (e.g. FC-unit-1) and unconformities are labelled consistently for all three sites because they are regional surfaces (e.g. UNC-1). Sediment was collected from the Fort Casey and Driftwood sites, whereby samples were recovered from fresh outcrop faces. At West Beach, sediment samples could only be collected at locations accessible by foot due to the steepness of the outcrop.

Grain size measurements were conducted by: (1) sieving the sediment at 500 µm; (2) measuring the fraction <500 µm with a Malvern 2000 grain-size analyzer; and (3) measuring the fraction >500 µm with a Retsch Technology Camsizer. Foreset slopes exposed in outcrops were measured using photomontages acquired via boat surveying, and a photomontage from Fort Casey was constructed using Washington State Coastal Atlas Shoreline Photos hosted by the Department of Ecology for the State of Washington.

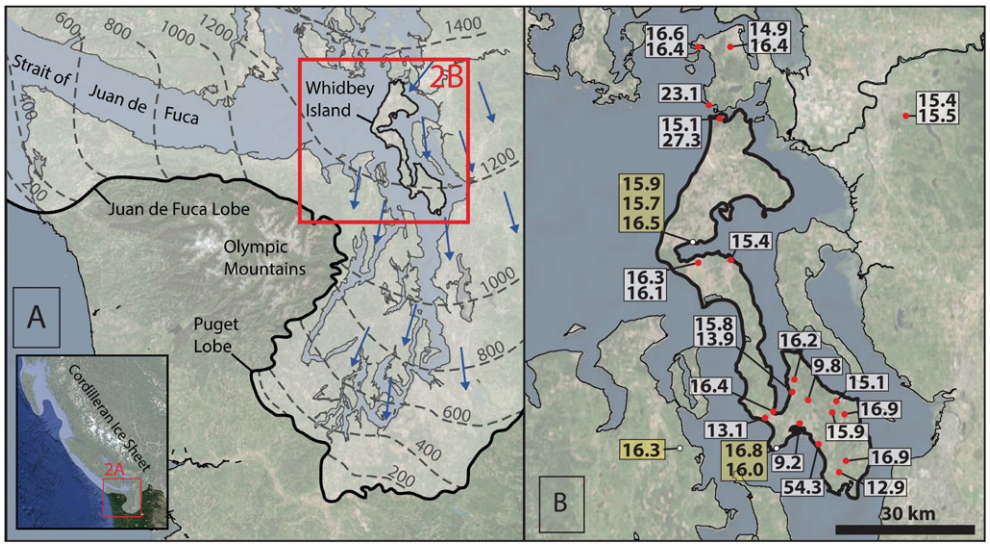

Figure 2. (A) Reconstruction of the maximum extent of the Fraser Glaciation into the Puget Lowlands. Dashed lines represent ice-thickness contours in meters (modified from Porter and Swanson, 1998). Blue arrows represent paleo-ice flow directions (Easterbrook, 2003). (B) Retreat chronology from and around Whidbey Island (bold, black outline). Exposure ages (36Cl) are sourced from bedrock and glacial erratics (red dots; Swanson and Caffee, 2001). Radiocarbon ages (white dots) are from shells sampled from the Everson Glacimarine Drift above the Vashon Till and organic material from lake sediments, which date the onset of marine incursion and subaerial landscape emergence, respectively (Leopold *et al.,* 1982; Anundsen *et al.,* 1994; Clague *et al.,* 1997; Swanson and Caffee, 2001). All ages are reported in thousand years before present. [Colour figure can be viewed at wileyonlinelibrary.com]

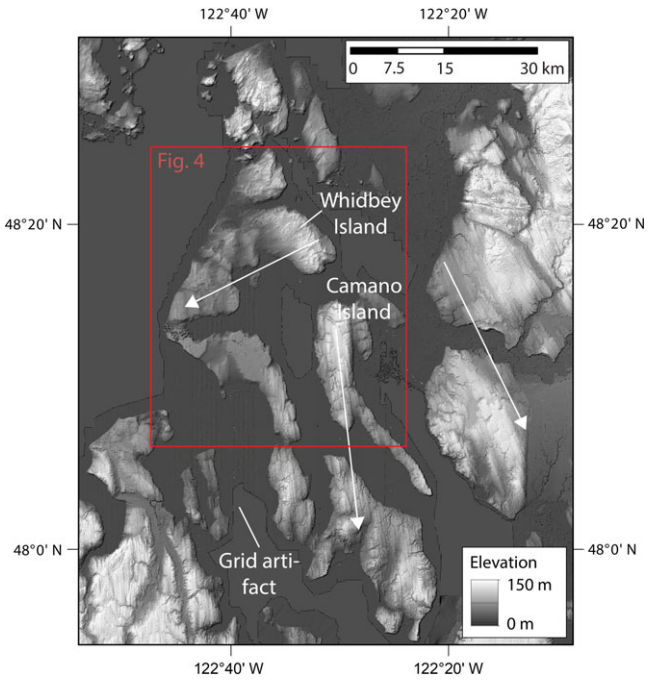

Figure 3. LIDAR imagery of Whidbey Island reveals streamlined glacial landforms with N–S and NE–SW orientations that record variable ice flow directions (indicated by arrows) (source: Puget Sound LIDAR Consortium, 6 ft spatial resolution). [Colour figure can be viewed at wileyonlinelibrary.com]

Results

Geomorphology

LIDAR imagery from across the Puget Lowlands reveals numerous landforms that are elongate with relatively uniform orientations and ridge spacing (Figure 3). Based on the morphology and dimensions of ridges and presence of lineations, these deposits are interpreted as formed in a subglacial environment (Clark, 1993; Stokes and Clark, 2002). Lineations are exposed in the modern surface topography, indicating formation during the most recent Vashon Stade glaciation, as they are typically covered by only a thin layer of Everson glacimarine sediments and other post-glacial deposits (e.g. soil and fluvial deposits). Some of the lineations on Whidbey Island meet the criteria to be classified as mega-scale glacial lineations (MSGLs), which requires linear forms with lengths of 10 000–100 000 m, elongation ratios exceeding 15:1, and convergent flow patterns (Clark, 1993; Stokes and Clark, 2002); other features do not meet these criteria, due to limited preservation or overprinting by other landforms. For simplicity, linear landforms will be referred to as lineations throughout the text. At the northern part of Whidbey Island, the lineations show a NE–SW orientation, and at the southern part of the island, the orientation is N–S (Figure 4). These two configurations could indicate a regional change in ice flow direction associated with the Juan de Fuca and Puget lobes (Figure 2(A)), or two different cross-cutting stages of flow, with the NE–SW oriented lineations overprinting N–S ice flow during deglacial ice retreat (Simkins *et al.,* 2017a).

Surface slope maps of Whidbey Island reveal asymmetric features oriented approximately perpendicular to lineations (Figure 4). Lidar data from Whidbey Island reveal that these features possess foreset slopes of 4–10°, exhibit sinuous topset-foreset crestlines, and are overprinted by lineations noted above (Figure 4). Distances between crestlines range from hundreds of meters to two kilometers. These features are tentatively interpreted as GZWs, given the strong geomorphological resemblance to known GZWs (Ottesen *et al.,* 2005; Dowdeswell *et al.,* 2016; Halberstadt *et al.,* 2016; Simkins *et al.,* 2016, 2017b) and internal stratigraphic architecture which reflects grounding zone processes, to be discussed in detail in later sections. In total, eleven GZWs have been recognized (five exposed in outcrop, six inferred based on geomorphic expression). Although the surficial landscape could have been significantly altered by glacial rebound and post-depositional alteration, the preservation of glacial landforms at the surface (Figure 3) indicates little erosion or significant burial of the surface topography by post-glacial deposits. Identification of GZWs on land is highly unusual; global-scale GZW studies, such as Batchelor and Dowdeswell (2015), do not document any such features. Thus, Whidbey Island deposits represent the first GZW outcrops to be presented in a peer-reviewed publication.

Outcrop sedimentology

Of the GZWs on Whidbey Island (Figure 4), the Fort Casey (FC), West Beach (WB) and Driftwood (DW) sites have well-preserved and accessible outcrops of diamictons with foreset beds. The internal sedimentary structures and the stratigraphic relationship between facies and their bounding surfaces at these sites were examined in detail to test whether the landform deposits are indeed consistent with previously documented GZW strata and morphology (Dowdeswell and Fugelli, 2012; Batchelor *et al.,* 2014; Batchelor and Dowdeswell, 2015; Simkins *et al.,* 2017b). Figure 5 shows photo-mosaics collected at the three outcrops, and Figure 6 shows representative measured sections for the Fort Casey and Driftwood outcrops, as well as down-section grain size distributions from the three sites.

Fort Casey

The Fort Casey outcrop is composed of six units and three unconformities (Figure 5(A) and 6(A1)). The basal unit at Fort Casey (FC-unit-1) is structureless diamicton that, coupled with its stratigraphic position, suggests FC-unit-1 is till associated with a glacial event that preceded the Vashon Stade (Figure 5(B)). FC-unit-1 is truncated by a fluvial erosional surface (UNC-1) and is overlain by non-glacial sediment deposits.

Table I. Whidbey Island outcrop and measured section locations, where northern (N) and southern (S) bounds of the photomontages are reported as latitude and longitude positions

Outcrop name	Photo mosaic location	Measured section location
Fort Casey (FC)	N: 48°10′36.52″N 122°41′16.22″WS: 48°10′27.44″N 122°41′10.38″ W	48°10′33.52″N 122°41′13.52″ W
Driftwood (DW)	N: 48°08′24.56″N 122°36′06.97″WS: 48°08′19.40″N 122°36′03.39″W	48°08′20.83″N 122°36′03.02″W
West Beach (WB)	N: 48°16′31.70″N 122°44′12.04″WS: 48°16′31.70″N 122°44′12.04″W	N/A

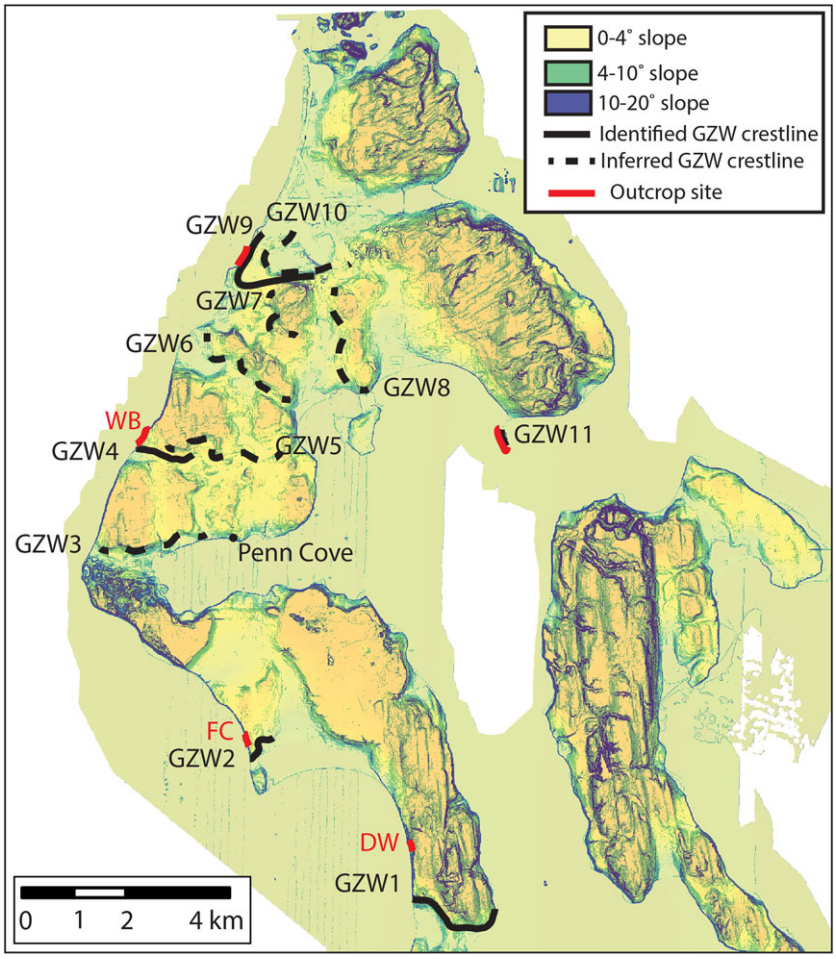

Figure 4. Map of surface slopes of Whidbey Island. Crestline orientations record episodic change in ice flow direction. Inferred GZW crestlines lack outcrop exposure. Outcrop locations are highlighted in red, with West Beach (WB), Fort Casey (FC), and Driftwood (DW) sections labelled. [Colour figure can be viewed at wileyonlinelibrary.com]

Non-glacial sediments include graded sands and conglomerates (FC-unit-2, -3, -4) composed of a horizontally bedded, shallowing-upward succession indicating a relative sea-level fall and, ultimately, subaerial exposure, as interpreted by the preservation of shoreface, beach and aeolian deposits (FC-unit-4). UNC-2 overlies and cuts into FC-unit-3 and -4, and is inferred to be a regional glacial erosional surface produced during the Vashon Stade advance of the southern Cordilleran Ice Sheet across Whidbey Island. FC-unit-1 through -4 are offset by a high-angle reverse fault that is truncated by UNC-2 (Figure 5(A)), likely a glacitectonic feature formed due to glacial over-riding and loading. Downlapping onto UNC-2 are prograding foresets composed mainly of discrete diamicton strata (FC-unit-5; Figure 7(A)) that locally show deformation features including rotated clasts. The foresets are interpreted as debris flow deposits. Measurements of individual foreset bed slopes range from 3 to 28°, consistent with the measured slopes based on the surface map created with the LIDAR data. Foreset beds of FC-unit-5 are interbedded with laterally discontinuous, cross-stratified sand and gravel and thinly laminated silt and clay with scattered dropstones (Figure 7(B)), interpreted as meltwater deposits and proximal glacimarine deposits, respectively. Less common deposits include horizontally bedded and well-sorted sand, silt and clay beds that lack dropstones, which are interpreted as sediment-laden gravity flow deposits. Foreset deposits are truncated by an irregular erosional surface (UNC-3) interpreted as a glacial unconformity (Figure 5(A)). Overlying UNC-3 is a massive diamicton that grades upwards into a pebbly mud (FC-unit-6) that varies laterally in thickness and is lithologically equivalent to FC-unit-1; this is interpreted as till. Grain-size data show upward fining and increasing sorting in FC-unit-6, identified as the Everson Glacimarine Drift (Figure 6(A1), (A2)).

West Beach

The West Beach outcrop contains four lithologic units and two unconformities (Figure 5(B)). The basal unit of the West Beach section (WB-unit-1, Figure 5(B)) is dominated by silt with scattered peat beds, indicating a shallow-water depositional environment. The WB-unit-1 is overlain by WB-unit-2, which consists of well-sorted sands with planar beds and low-angle cross–beds that are interpreted as aeolian deposits. WB-unit-1 and -2 were likely deposited during a period of relative sea-level fall, similar to FC-unit-2 through -4 of the Fort Casey succession. WB-unit-1 and -2 are cut by an irregular erosional surface, interpreted to be the regional glacial unconformity UNC-2 associated with the Vashon Stade advance. The pre-Vashon Stade fluvial erosion surface, UNC-1, is not exposed at this outcrop. UNC-2 exhibits significant relief and is interpreted as a paleo-glacial trough flank based on the relief on this surface and overlying interpreted GZW deposits. Above UNC-2 are diamictons (WB-unit-3) that indicate progradation to the S-SW. WB-unit-3 is truncated by another glacial erosional surface (UNC-3; Figure 5(B)). Overlying UNC-3 is a massive diamicton (WB-unit-4) which is interpreted as till. WB-unit-4 grades from diamicton at the base to pebbly mud at the top. Access for sampling is limited at this outcrop, so only the top portion of WB-unit-4 was sampled. Grain-size data indicate moderate sorting

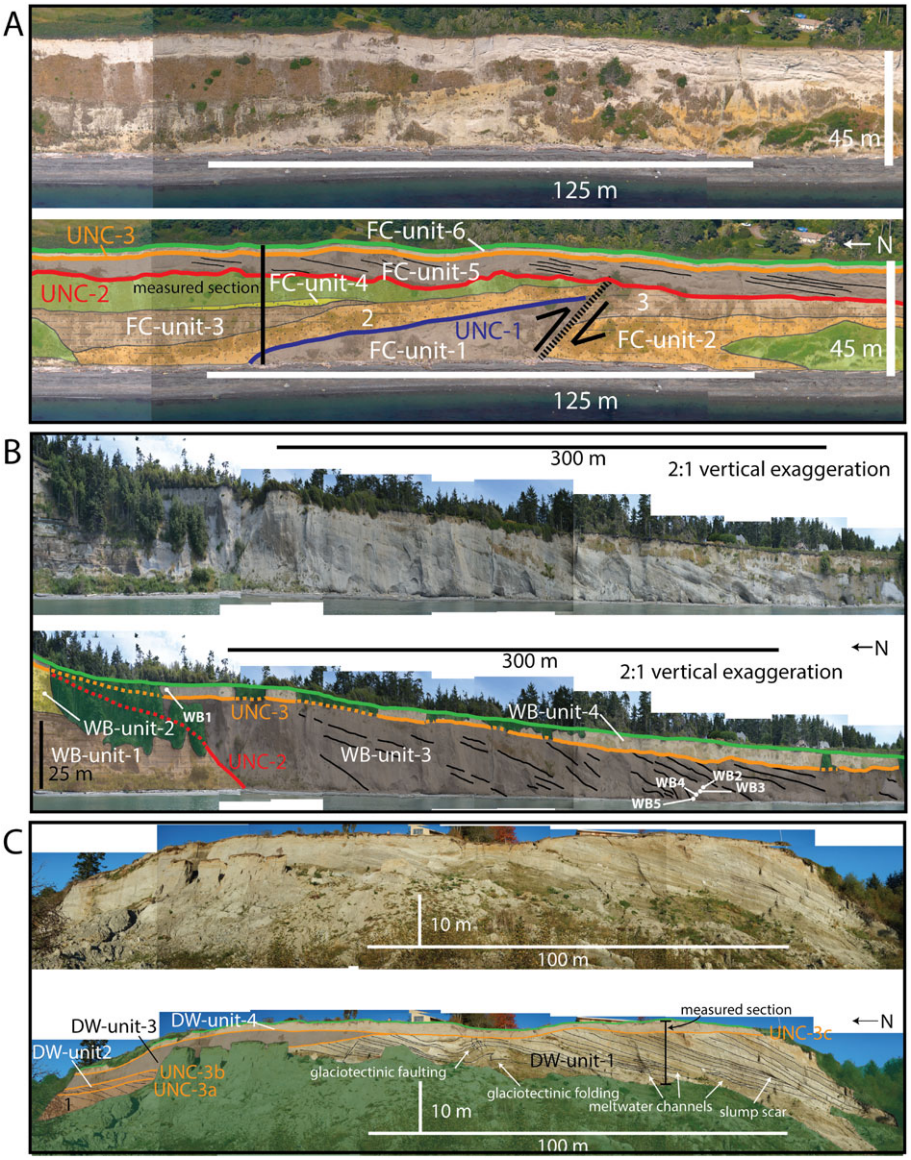

Figure 5. (A) Fort Casey section: glacitectonic thrust faulting exposes Pre-Vashon Stade diamicton (FCunit-1). Fluvial erosional surface (UNC-1) underlies an interglacial shallowing-upward succession (FC-units-2, 3, and 4). Undulatory erosional surface UNC-2 (red line) is interpreted to be the regional glacial erosional surface associated with Vashon Stade advance. Downlapping onto UNC-2 are southward prograding diamictons (FC-unit-5) interpreted as GZW foreset deposits. Undulatory erosional surface UNC-3 truncates FC-unit-5 and is interpreted to be a localized re-advance surface formed through GZW development. UNC-3 is capped by a deformation till (FC-unit-6) that fines upward into draping glacimarine sediment (green line). (B). West Beach section: WB-unit-1 and -2 represent a shallowing upward sequence, capped by a highly undulatory erosional surface (UNC-2) interpreted to be the regional glacial erosional surface associated with Vashon Stade advance, similar to Fort Casey. WB-unit-3 is a prograding diamicton interpreted to be GZW foresets. Truncating WB-unit-3 is UNC-3, a localized re-advance surface. Overlying UNC-3 is a deformation till (WB-unit-4) that is draped by glacimarine sediment (green line). (C) Driftwood section: DW-units-1 and -2 are comprised of meltwater channel deposits, meltwater plume deposits, and sediment gravity flow deposits ranging from turbidites to matrix-supported debris flows. Between DW-unit-1 and -2 is an unconformity (UNC-3a) interpreted to be a localized re-advance surface. An additional re-advance (UNC-3b) surface truncates DW-unit-2. DW-unit-3 is a diamicton interpreted to be a deformation till, bracketed by re-advance surfaces UNC-3b and UNC-3c. Above UNC-3c is a deformation till that is draped in glacimarine sediment (green line). The presence of multiple localized re-advance surfaces indicates that this outcrop represents a composite GZW. [Colour figure can be viewed at wileyonlinelibrary.com]

associated with a relatively high volume of fine sediment, indicating greater marine influence upward in the section (Figure 6(B)).

Driftwood section

The Driftwood Outcrop exposes mostly progradational diamictons and the basal glacial unconformity (UNC-2) is not exposed at this site (Figure 5(C)). The northern part of the section includes two southward-prograding units that are separated by an erosional surface, suggesting the presence of two stacked GZWs. The lower unit (DW-unit-1) thickens to the south, where individual foreset beds measure up to 15 m in height. DW-unit-1 is overlain by an undulatory erosional surface (UNC-3a). DW-unit-2 is also comprised of distinct foreset beds which pinch out due to the overlying erosional surface UNC-3b. The lower unit (DW-unit-3) is composed mainly of structureless diamicton and overlain by an undulatory erosional surface (UNC-3c). Unlike the Fort Casey and West Beach exposures, the progradational section of the Driftwood outcrop contains a diverse assortment of sedimentary facies, including diamictons, laterally discontinuous conglomerates and sands with trough cross-bedding, and thinly laminated sand, silt, and clay beds with interspersed dropstones (Figure 7(C)). There are also pervasive glacitectonic structures within the section such as soft sediment folds and thrusts (Figure 7(D)). This is also the only location where potential tidal deposits exist, identified

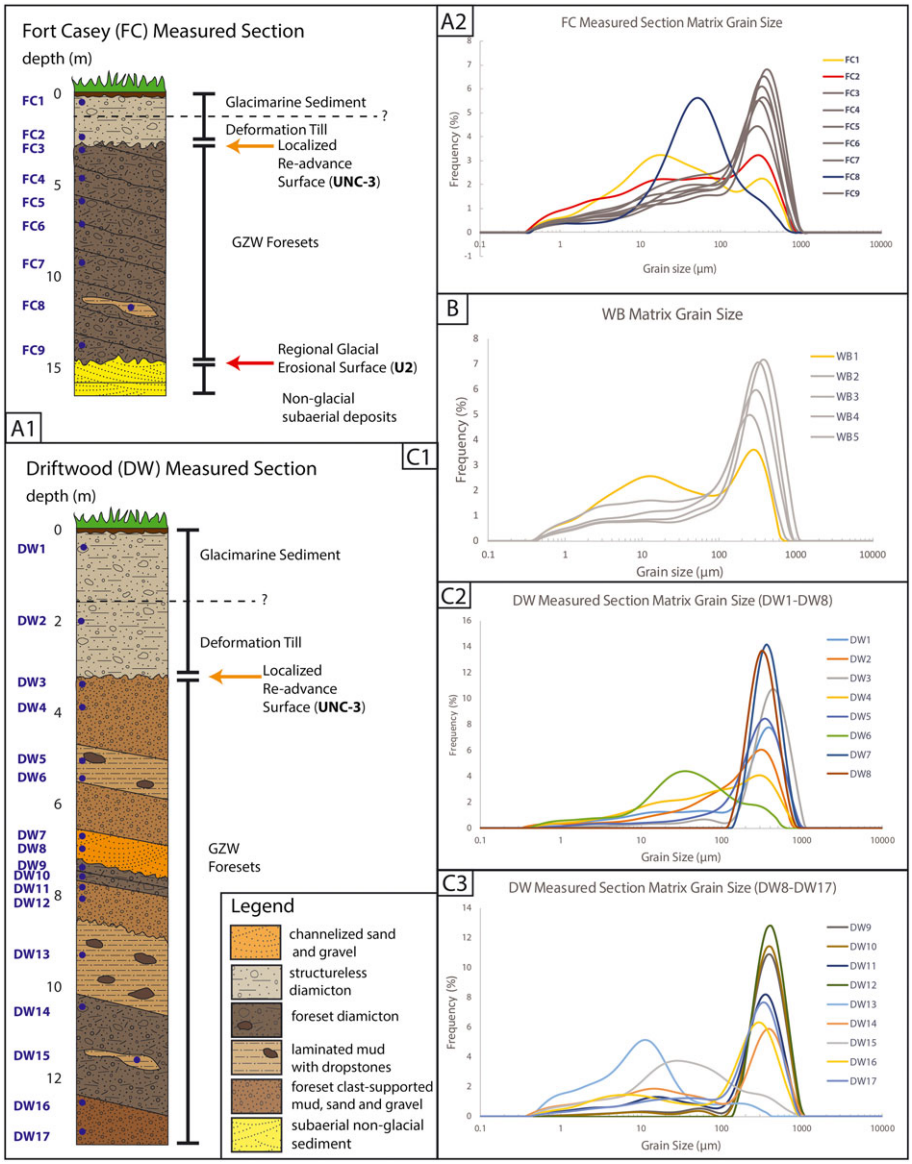

Figure 6. (A1) Fort Casey section stratigraphic column. Blue dots represent sample locations. (A2) Grainsize distributions for samples corresponding to sample locations shown in (A1). (B) Grainsize distributions for WB samples. See Figure 5(B) for sample locations. (C1). Driftwood section stratigraphic column. Blue dots represent sample locations. (C2), (C3) Grainsize distributions for samples shown in (C1). [Colour figure can be viewed at wileyonlinelibrary.com]

by alternating, laminated sands and muds (Figure 7(E)); however, bedforms indicating bidirectional transport are not observed. The Driftwood section demonstrates a compelling example of erosion into underlying foreset beds, overlain by a second package of foresets (Figure (5C)). DW-unit-3 is a massive diamicton that contains glacitectonic features. DW-unit-3 is interpreted as deformation till that was deposited by ice over-riding the wedge. DW-unit-4 is a massive diamicton, interpreted to be a deformation till at its base. DW-unit-4 is capped by glacimarine deposits of Everson Drift that display upward fining and decreased clast content.

Discussion

GZW morphology and stratigraphy

The main difference between recessional moraines and GZWs is that the latter require flowing ice, and record grounding line stability and subsequent re-advance, as evidenced by prograding foreset deposits, erosion of wedge surfaces and/or lineations that extend across wedge surfaces (Sexton *et al.,* 1992; Mosola and Anderson, 2006; Ottesen *et al.,* 2007; Dowdeswell and Fugelli, 2012). The interpreted GZWs on Whidbey Island exhibit most, if not all, of these characteristics. They also possess asymmetric morphologies and sinuous crestlines that are oriented roughly perpendicular to the paleo-ice flow direction of the southern Cordilleran Ice Sheet (Figure 3).

Field observations at three outcrops indicate that the GZWs are composed mainly of diamictons and have topsets and foresets bounded by upper and lower unconformities. For example, the crestline of GZW1 extends across Whidbey Island, outcropping on both the eastern and western sides, and contains southward prograding foreset beds bounded by glacial unconformities (Figure 4). Progradation over a lower unconformity and truncation by an upper unconformity is consistent with observations of GZWs from high-latitude continental shelves (Anderson, 1999; Li *et al.,* 2011; Dowdeswell and Fugelli, 2012).

The Whidbey Island GZWs range from (10^0–10^2 m) in height and (10^2–10^4 m) in width (Figure 8). This is smaller than wedges originally imaged on high-latitude continental shelves using seismic and multibeam data (Shipp *et al.,* 1999; Ottesen

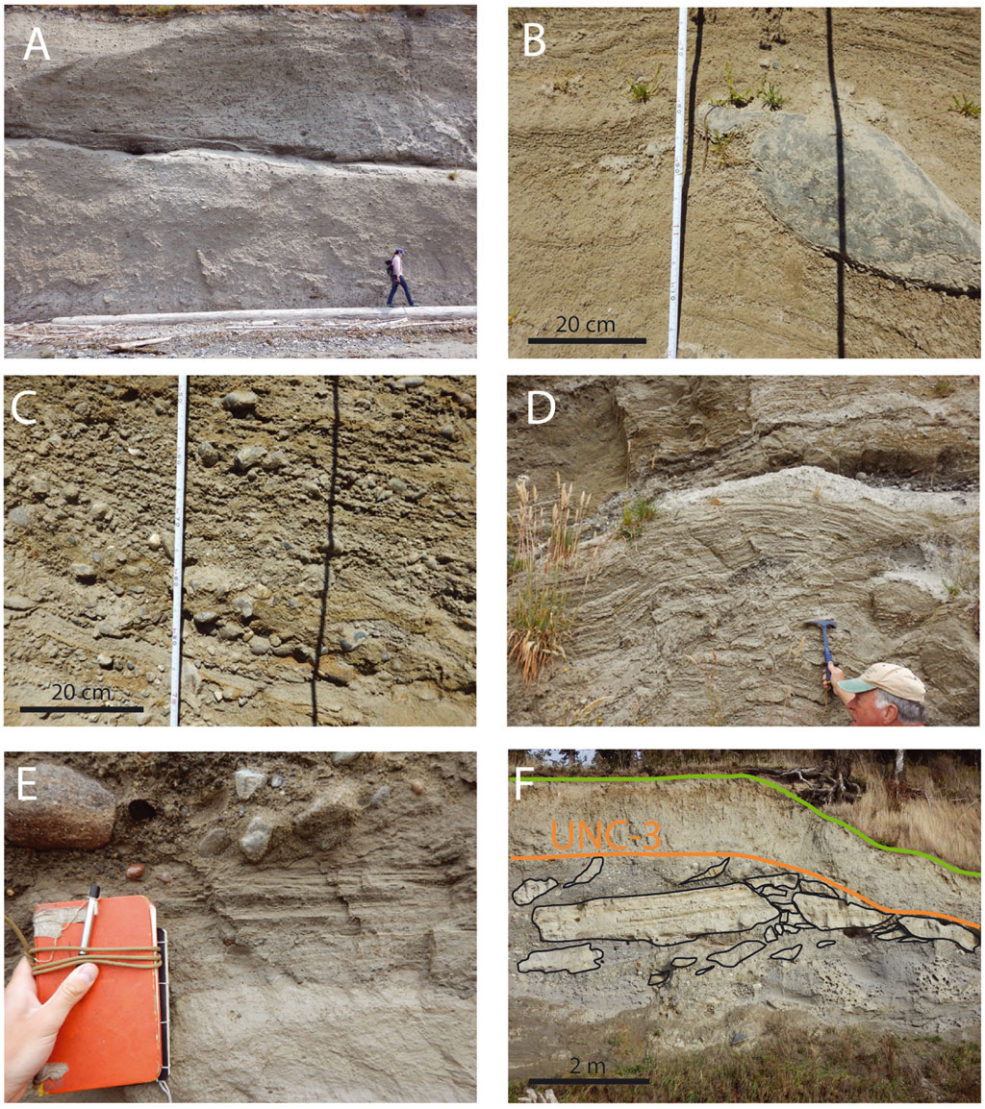

Figure 7. (A) Prograding diamictons interpreted to be debris flow deposits with fine-grained turbidite and suspension fallout interbeds. (B) Laminated silt and sand with dropstones. (C) Cross-stratified sands and conglomerates. (D) Glacitectonic deformation of sediment (E) Sand–silt couplets serve as evidence for tidal currents mobilizing sediment at the grounding line. (F) Mega-breccia clasts (outlined in black) and sandy gravel conglomerates truncated by a localized re-advance surface (UNC-3) and capped by deformation till that fines upward into glacimarine sediment. [Colour figure can be viewed at wileyonlinelibrary.com]

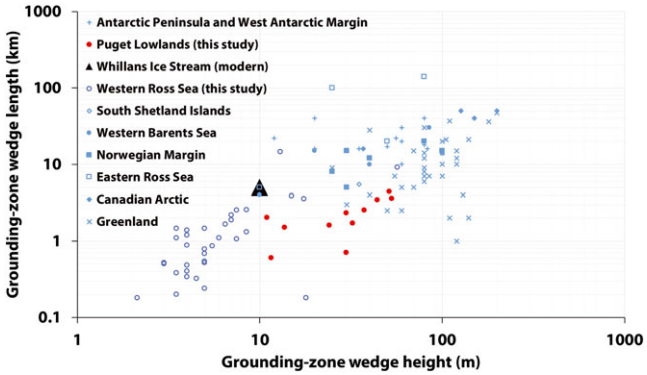

Figure 8. GZW height vs GZW length. The black triangle represents the modern Whillans Ice Stream GZW. Whidbey Island GZWs fall within the size range of previously studied GZWs from other glaciated margins (Anandakrishnan *et al.,* 2007; Simms *et al.,* 2011; Bart and Cone, 2012; Simkins *et al.,* 2018). [Colour figure can be viewed at wileyonlinelibrary.com]

et al., 2005; Mosola and Anderson, 2006; Li *et al.,* 2011; Dowdeswell and Fugelli, 2012; Dowdeswell *et al.,* 2014; Batchelor and Dowdeswell, 2015; Bart *et al.,* 2017). However, recent research efforts in the Ross Sea utilizing an advanced high-resolution multibeam imaging system have revealed numerous GZWs of the size range measured on Whidbey Island that were otherwise unresolvable with previous technology (Halberstadt *et al.,* 2016; Simkins *et al.,* 2017b, 2018), (Figure 8). The extent of foreset progradation exhibited by Whidbey Island wedges ranges from hundreds of meters to roughly two kilometers, indicating that episodes of grounding line re-advance of this magnitude occurred during overall retreat of the southern Cordilleran Ice Sheet.

Sedimentary processes as revealed by GZW outcrops

Previous researchers hypothesized that GZWs are nourished by deformation till and debris transported in the basal portion of the ice sheet to the grounding line, as a line-source of sediment, so that the deposit progrades in the direction of ice flow (Alley *et al.,* 1986, 1989). These early models envisioned wedge accumulation within depressions that provided accommodation space for their development. However, later observations of

GZW stratal patterns using high-resolution seismic data revealed aggradational stacking of foreset beds (Anderson, 1999), and even stacking of wedges to form composite wedges (Howat and Domack, 2003; Bart *et al.,* 2017), indicating both horizontal and vertical wedge growth. Wedge geometry and increasing foreset height indicate that accommodation space for sediment accumulation increases in the direction of flow. Hence, GZWs are constructional features that aggrade at the grounding line, where ice thickness decreases, until buoyancy limits are exceeded and the grounding line rapidly shifts landward (Simkins *et al.,* 2018).

Growth of GZWs is ultimately controlled by sediment flux to the grounding line, which as previously noted is difficult to constrain both in space and time. Simkins *et al.* (2018) identified a general pattern of increasing GZW sinuosity with increasing wedge amplitude, which is attributed to variations in sediment accumulation along the grounding line. They further argue that these differences are largely controlled by subglacial hydrology, specifically dispersive versus channelized flow, which impacts both bed erosion and sediment transport. In general, channelized meltwater flow results in variable sediment supply to the grounding line and produces embayments where meltwater erosion and tidal forces may contribute to grounding line instability (Simkins *et al.,* 2017b).

While sediment flux to the grounding line is key to GZW construction, we are restricted by outcrop studies to examining processes responsible for transporting sediments to and seaward of the grounding line. The GZW diamictons at the West Beach and Fort Casey sections indicate that a viscous, matrix-supported sediment was transported downslope via debris flows, accumulating to construct foreset beds, whereby individual events are separated by thin beds of finely laminated sand and mud lacking ice-rafted material (Figure 7(A)). These laminated deposits are interpreted as suspension fallout and/or turbidites, possibly associated with sediment-enriched meltwater discharge from beneath the ice. Otherwise, little evidence for depositional processes other than mass movement are preserved in these outcrops. This could be a result of: (1) the diagnostic similarities between structureless debris flow diamicton and proximal glacimarine deposits (Kurtz and Anderson, 1979), and/or (2) continuous remobilization of various facies by debris flow processes throughout GZW development.

In contrast to the West Beach and Fort Casey exposures, foreset deposits at the Driftwood section include a variety of sedimentary facies and associated depositional processes. Poorly sorted mixtures of mud, sand and gravel are interbedded with sorted sands with trough cross-stratification (Figure 7(C)). These deposits are interpreted to originate from meltwater flows that maintained shear stress sufficient to erode the underlying foresets. Other prominent foreset deposits are laminated, sorted mud and sand that contain dropstones and drapes underlying deposits (Figure 7(B)). These are interpreted to arise from fallout of entrained basal sediment, with some of the draping fine material possibly being sourced from settling of sediment suspended in meltwater plumes. Draping sorted mud and sand containing dropstones (Figure 7B) are common at the Driftwood outcrop (Figure 6(C1)). These interpretations indicate that the Driftwood section was proximal to a meltwater outlet. Subglacial channel deposits are also exposed on Whidbey Island, specifically as mega-breccias that underlie the Everson Drift at locations around Penn Cove (Simkins *et al.,* 2017a; Figure 3, Figure 7(F)).

Well-sorted, thinly-bedded sand and mud couplets occur within some channel packages at the Driftwood location (Figure 7(E)). These are interpreted as tidal deposits. This is consistent with the supposition that tidal movement of sediment-laden water into and out of subglacial cavities occurs at the grounding line (Anandakrishnan *et al.,* 2003; Horgan *et al.,* 2013). The co-existence of meltwater channels and tidal deposits implies that the Driftwood location may have been an embayment in the grounding line, which is consistent with the occurrence of meltwater channel deposits (Horgan *et al.,* 2013; Simkins *et al.,* 2017b).

At all accessible locations, there is a glacial unconformity above the GZW with lineations characterizing the landscape surface (Figure 3). This indicates re-advance of the grounding line, similar to what is observed in GZWs of Antarctica's glaciated margins, such as the Mertz Trough, East Antarctica (McMullen *et al.,* 2016), the Ross Sea (Mosola and Anderson, 2006; Bart and Cone, 2012; Halberstadt *et al.,* 2016; Bart *et al.,* 2017; Simkins *et al.,* 2018), and Pine Island Bay (Jakobsson *et al.,* 2012). In all these areas, MSGLs extend across the surfaces of GZWs. On Whidbey Island, however, overriding glacial unconformities extend beyond the crestline of the GZWs and over the foreset slope of these landforms. It is thus inferred that the GZWs of Whidbey Island were overridden by local ice re-advancement, indicating that ice thickness relative to water depth was sufficient to inhibit ice floating at these locations. This is perhaps a result of isostatic uplift during ice retreat.

The GZWs of Whidbey Island are capped by Everson Drift, which is a glacimarine facies that is characterized by a range of sediment types, including diamictons that are interpreted as having been deposited in close proximity to the grounding line, and pebbly mudstones that are deposited farther from the ice margin. There is evidence of increased marine influence moving upwards within the glacimarine section in the form of improved grain-size sorting (Figure 6) and increased presence of marine fossils.

Retreat patterns and styles as inferred by GZW deposits

Retreat of the southern Cordilleran Ice Sheet is argued to have been triggered by marine incursion through the Strait of Juan de Fuca, causing the ice to decouple from the seafloor and rapidly disintegrate (Easterbrook, 1986, 2003). This implies a low profile ice sheet. However, the occurrence of the GZWs on Whidbey Island (five exposed in outcrop, six inferred based on geomorphic expression) indicates that retreat was punctuated, and that pauses were sufficiently long to provide the time to produce GZWs. This style of retreat is more consistent with the bedrock relief and geology of the region, which would have provided numerous pinning points for the retreating ice sheet. Additionally, high basal melt rates will enhance englacial debris deposition at the grounding zone, and the observation of such deposits in the form of the Everson drift draping Whidbey Island indicates relatively lower melt rates that could correspond to slower retreat.

Ice sheet margin stability is dependent on the relationship between ice thickness and water depth. An important component facilitating ice sheet margin stability is GZW growth, which reduces local water depth and, assuming consistent ice sheet thickness, limits ice floating and detachment from the bed (Alley *et al.,* 2007). Alternative processes in which favorable local water depth or ice thickness initiates nucleation and growth of a GZW can also occur. The full extent to which GZWs influence ice sheet margin stability remains unconstrained, yet it is evident that the formation of a GZW triggers a feedback whereby GZW growth acts to stabilize the grounding line.

The rate of sediment supply to the grounding line and available accommodation space play important roles in setting the duration of grounding line stability. At the West Beach outcrop, GZW foresets fill accommodation space in the form of a low in the antecedent topography (Figure 5(B)). The Fort Casey GZW rests on a surface that slopes gently in the direction of progradation (Figure 5(A)). The basal unconformity of the Driftwood GZW is not exposed, but overall stacking patterns are aggradational (Figure 5(C)). The upper surfaces of all three GZWs were eroded, so actual surface morphologies have been removed, but the presence of these three wedges indicates the possibility of prolonged stability and localized re-advance of ice overtop of the deposit.

Sediment flux at the ice grounding line remains poorly constrained, so it is difficult to use the size of the GZW to estimate the time duration of ice sheet margin stability. For example, rapid basal melting of sediment-laden ice would cause a pulse of sediment deposition, immediately increasing GZW size. Nevertheless, the geometry of, and spacing between, adjacent GZWs can be used to characterize retreat events. One would expect that larger GZWs coincide with longer time periods of ice sheet margin stability; additionally, greater distance between adjacent GZWs likely reflects relatively rapid rates of ice retreat (Alley *et al.,* 2007; Dowdeswell *et al.,* 2008; Simkins *et al.*, 2018). Crestline spacing of wedges decreases from south to north, from several kilometers (GZW1 to GZW2) to hundreds of meters (GZW9 to GZW10), (Figure 4), suggesting that the rate of grounding line retreat decreased toward the north where greater bedrock exposure and higher relief could have provided pinning points to stabilize the ice sheet. In general, the location of the Whidbey Island GZWs appear to associate with topographic pinning points, which occur as both bedrock and paleo-sedimentary highs.

Estimates of GZW formation range from decades to thousands of years (Alley *et al.,* 2007; Anandakrishnan *et al.,* 2007; Dowdeswell *et al.,* 2008; Simkins *et al.,* 2018). The Whidbey Island wedges are similar in size to those of the western Ross Sea (Figure 8), where estimates of wedge formation range from decades to centuries (Simkins *et al.,* 2018). In turn, the Whidbey Island wedges may have formed over similar time scales. This assessment is not inconsistent with existing radiocarbon and ^{36}Cl exposure-age chronologies, which indicate that grounding line retreat across Whidbey Island may have occurred over several centuries (Easterbrook, 1986, 1994; Swanson and Caffee, 2001). This assessment indicates, therefore, a punctuated style of retreat of the southern Cordilleran Ice Sheet, based on the occurrence of eleven GZWs mapped on Whidbey Island.

Conclusions

Multiple locations where diamictons possess foreset stratification showing varying degrees of preservation are recognized on Whidbey Island, Washington; these packages are bounded by glacial unconformities and overprinted by lineations. These landforms are interpreted as GZWs, which accumulated during pauses in overall grounding line retreat of the Puget Ice Lobe. GZW progradation distances indicate grounding line advances on the order of hundreds of meters and up to two kilometers.

Outcropping GZW foresets contain a variety of deposits and reflect a range of transport processes, but the dominance of diamictons indicates that the prevailing transport mode was debris flows. The Driftwood outcrop is unique in that it yields evidence for basal melt-out of entrained debris, channelized meltwater flows and tidal activity.

GZW foresets are truncated by localized re-advance surfaces and, in the Fort Casey and West Beach sections, deposits downlap onto a regional glacial erosional surface associated with the Vashon Stade advance. These stratigraphic characteristics correspond to seismically resolved surfaces within GZWs observed in Antarctica and Greenland (Anderson, 1999; Dowdeswell and Fugelli, 2012; Batchelor and Dowdeswell, 2015). This is supported by outcrop observations of deformation till deposited along topsets that truncates foresets, creating a localized re-advance surface, which is then draped in glacimarine sediment after abandonment of the GZW.

Ice retreat across Whidbey Island is marked by eleven backstepping grounding lines, as identified in both topographic maps and field reconnaissance. Available chronostratigraphic data from the Puget Lowlands supports the assessment that back-stepping could have occurred over decadal to centennial time scales. The Whidbey Island GZWs provide compelling evidence of local ice advance during GZW formation, which supports stabilizing feedbacks on ice sheet grounding lines due to the growth of these landforms.

Acknowledgements—We thank Andrew Moodie and Josh Crozier for assistance in the field, and the Whidbey Camano Land Trust, namely Patricia Powell, for providing access to key outcrops. The University of Washington is also thanked for providing access to a small boat in order to conduct field surveys. Our research was partially supported by the National Science Foundation Office of Polar Programs grant NSF/ARRA ANT-0837925 to J.B.A.

References

Alley RB, Anandakrishnan S, Dupont TK, Parizek BR, Pollard D. 2007. Effect of sedimentation on ice-sheet grounding-line stability. *Science* **315**: 1838–1841. https://doi.org/10.1126/science.1138396.

Alley RB, Blankenship DD, Bentley CR, Rooney ST. 1986. Deformation of till beneath Ice Stream B, West Antarctica. *Nature* **322**: 57–59. https://doi.org/10.1038/322057a0.

Alley RB, Blankenship DD, Bentley CR, Rooney ST. 1987. Till beneath ice stream B. 3. Till deformation: evidence and implications. *Journal of Geophysical Research* **92**: 8921–8929. https://doi.org/10.1029/JB092iB09p08921.

Alley RB, Blankenship DD, Rooney ST, Bentley CR. 1989. Sedimentation beneath ice shelves—the view from Ice Stream B. *Marine Geology* **85**: 101–120. https://doi.org/10.1016/0025-3227(89) 90150-3.

Anandakrishnan S, Catania GA, Alley RB, Horgan HJ. 2007. Discovery of till deposition at the grounding line of Whillans Ice Stream. *Science* **315**: 1835–1838. https://doi.org/10.1126/science.1138393.

Anandakrishnan S, Voigt DE, Alley RB, King MA. 2003. Ice stream D flow speed is strongly modulated by the tide beneath the Ross Ice Shelf. *Geophysical Research Letters* **30**: 1361. https://doi.org/10.1029/2002GL016329.

Anderson JB. 1999. *Antarctic Marine Geology*. Cambridge University Press: New York, NY.

Anderson JB, Jakobsson M. 2017. Grounding-zone wedges on the Antarctic continental shelves. In *Atlas of Submarine Glacial Landforms: Modern, Quaternary and Ancient*, Dowdeswell JA, Canals M, Jakobsson M, Todd BJ, Dowdeswell EK, Hogan KA (eds). Geological Society of London, Memoirs 46: London; 3–14 https://doi.org/10.1144/M46.171.

Anundsen K, Abella S, Leopold E, Stuiver M, Turner S. 1994. Late glacial and early Holocene sea-level fluctuations in the central Puget Lowland, Washington, inferred from lake sediments. *Quaternary Research* **42**: 149–161. https://doi.org/10.1006/qres.1994.1064.

Armstrong JE, Crandell DR, Easterbrook DJ, Noble JB. 1965. Late Pleistocene stratigraphy and chronology in southwestern British Columbia and northwestern Washington. *Geological Society of America Bulletin* **76**: 321–330. https://doi.org/10.1130/0016-7606(1965)76[321:LPSACI]2.0.CO;2.

Bart PJ, Anderson JB, Nitsche F. 2017. Post-LGM grounding-line positions of the Bindschadler Paleo Ice Stream in the Ross Sea

Embayment, Antarctica. *Journal of Geophysical Research, Earth Surface* **122**: 1827–1844. https://doi.org/10.1002/2017JF004259.

Bart PJ, Cone AN. 2012. Early stall of West Antarctic Ice Sheet advance on the eastern Ross Sea middle shelf followed by retreat at 27,500 C-14 yr BP. *Palaeogeograhy Palaeoclimatology Palaeoecology* **335**: 52–60. https://doi.org/10.1016/j.palaeo.2011.08.007.

Bart PJ, Owolana B. 2012. On the duration of West Antarctic Ice Sheet grounding events in Ross Sea during the Quaternary. *Quaternary Science Reviews* **47**: 101–115. https://doi.org/10.1016/j.quascirev.2012.04.023.

Batchelor CL, Dowdeswell JA. 2015. Ice-sheet grounding-zone wedges (GZWs) on high-latitude continental margins. *Marine Geology* **363**: 65–92. https://doi.org/10.1016/j.margeo.2015.02.001.

Batchelor CL, Dowdeswell JA, Pietras JT. 2014. Evidence for multiple Quaternary ice advances and fan development from the Amundsen Gulf cross-shelf trough and slope, Canadian Beaufort Sea margin. *Marine and Petroleum Geology* **52**: 125–143. https://doi.org/10.1016/j.marpetgeo.2013.11.005.

Booth DB, Troost KG, Clague JJ, Waitt RB. 2003. The Cordilleran Ice Sheet. *Developments in Quaternary Science* **1**: 17–43. https://doi.org/10.1016/S1571-0866(03)01002-9.

Christoffersen P, Tulaczyk S, Behar AE. 2010. Basal ice sequences in Antarctic ice stream: exposure of past hydrologic conditions and a principle mode of sediment transfer. *Journal of Geophysical Research* **115**: 1–12. https://doi.org/10.1029/2009JF001430.

Clague JJ, James TS. 2002. History and isostatic effects of the last ice sheet in southern British Columbia. *Quaternary Science Reviews* **21**: 71–87. https://doi.org/10.1016/S0277-3791(01)00070-1.

Clague JJ, Mathewes RW, Guilbault JP, Hutchinson I, Rickets BD. 1997. Pre-Younger Dryas resurgence of the southwestern margin of the Cordilleran Ice Sheet, British Columbia, Canada. *Boreas* **26**: 261–277. https://doi.org/10.1111/j.1502-3885.1997.tb00855.x.

Clark CD. 1993. Mega-scale glacial lineations and cross-cutting ice-flow landforms. *Earth Surface Processes and Landforms* **18**: 1–29. https://doi.org/10.1002/esp.3290180102.

DeConto RM, Pollard D. 2016. Contribution of Antarctica to past and future sea-level rise. *Nature* **531**: 591–597. https://doi.org/10.1038/nature17145.

Domack EW. 1983. Facies of late Pleistocene glacial-marine sediments on Whidbey Island, Washington—an isostatic glacial-marine sequence. In *Glacial-marine Sedimentation*, Molnia BF (ed). Plenum Press: New York; 535–570.

Dowdeswell JA, Canals M, Jakobsson M, Todd BJ, Dowdeswell EK, Hogan KA. 2016. The variety and distribution of submarine glacial landforms and implications for ice-sheet reconstruction. *Geological Society, London, Memoirs* **46**: 519–552. https://doi.org/10.1144/M46.183.

Dowdeswell JA, Fugelli EMG. 2012. The seismic architecture and geometry of grounding-zone wedges formed at the marine margins of past ice sheets. *Geological Society of America Bulletin* **124**: 1750–1761. https://doi.org/10.1130/B30628.1.

Dowdeswell JA, Hogan KA, Ó Cofaigh C, Fugelli EMG, Evans J, Noormets R. 2014. Late Quaternary ice flow in a West Greenland fjord and cross-shelf trough system: submarine landforms from Rink Isbrae to Uummannaq shelf and slope. *Quaternary Science Reviews* **92**: 292–309. https://doi.org/10.1016/j.quascirev.2013.09.007.

Dowdeswell JA, Ottesen D, Evans J, Cofaigh CÓ, Anderson JB. 2008. Submarine glacial landforms and rates of ice-stream collapse. *Geology* **36**: 819–822. https://doi.org/10.1130/G24808A.1.

Easterbrook DJ. 1963. Late Pleistocene glacial events and relative sea-level changes in the northern Puget Lowland, Washington. *Geological Society of America Bulletin* **74**: 1465–1484. https://doi.org/10.1130/0016-7606(1963)74[1465:LPGEAR]2.0.CO;2.

Easterbrook DJ. 1986. Stratigraphy and chronology of Quaternary deposits of the Puget Lowland and Olympic Mountains of Washington and the Cascade Mountains of Washington and Oregon. In *Quaternary Glaciations in the Northern Hemisphere*, Sibrava V, Bowen DQ, Richmond GM (eds). Pergamon Press: New York; 514.

Easterbrook DJ. 1994. Chronology of pre-late Wisconsin Pleistocene sediments in the Puget Lowland, Washington. *Washington Division of Geology and Earth Resources Bulletin* **80**: 191–206.

Easterbrook DJ. 2003. Cordilleran Ice Sheet glaciation of the Puget Lowland and Columbia Plateau and alpine glaciation of the North Cascade Range, Washington. *Geological Society of America Field Guide* **4**: 137–157.

Golledge NR, Kowalewski DE, Naish TR, Levy RH, Fogwill CJ, Gasson EG. 2015. The multi-millennial Antarctic commitment to future sea-level rise. *Nature* **526**: 421–425. https://doi.org/10.1038/nature15706.

Halberstadt A, Simkins L, Greenwood S, Anderson JB. 2016. Past ice-sheet behavior: retreat scenario and changing controls in the Ross Sea, Antarctica. *The Cryosphere* **10**: 1003–1020. https://doi.org/10.5194/tc-10-1003-2016.

Hodson TO, Powell RD, Brachfeld SA, Tulaczyk S, Scherer RP, Team WS. 2016. Physical processes in subglacial Lake Whillans, West Antarctica: inferences from sediment cores. *Earth and Planetary Science Letters* **444**: 56–63. https://doi.org/10.1016/j.epsl.2016.03.036.

Horgan HJ, Christianson K, Jacobel RW, Anandakrishnan S, Alley RB. 2013. Sediment deposition at the modern grounding zone of Whillans Ice Stream, West Antarctica. *Geophysical Research Letters* **40**: 3934–3939. https://doi.org/10.1002/grl.50712.

Howat IM, Domack EW. 2003. Reconstructions of western Ross Sea palaeo-icestream grounding zones from high-resolution acoustic stratigraphy. *Boreas* **32**: 56–75. https://doi.org/10.5194/tc-2016-33.

Jakobsson M, Anderson JB, Nitsche FO, Gyllencreutz R, Kirshner AE, Kirchner N, O'Regan M, Mohammad R, Eriksson B. 2012. Ice sheet retreat dynamics inferred from glacial morphology of the central Pine Island Bay Trough, West Antarctica. *Quaternary Science Reviews* **38**: 1–10. https://doi.org/10.1016/j.quascirev.2011.12.017.

King LH, Rokoengen K, Fader GBJ, Gunleiksrud T. 1991. Till-tongue stratigraphy. *Geological Society of America Bulletin* **103**: 637–659. https://doi.org/10.1130/0016-7606(1991)103<0637:TTS>2.3.CO;2.

Kurtz DD, Anderson JB. 1979. Recognition and sedimentologic description of recent debris flow deposits from the Ross and Weddell Seas, Antarctica. *Journal of Sedimentary Petrology* **49**: 1159–1170. https://doi.org/10.1306/212F78D8-2B24-11D7-8648000102C1865D.

Leopold EB, Nickmann R, Hedges JI, Ertel JR. 1982. Pollen and lignin records of late Quaternary vegetation, Lake Washington. *Science* **218**: 1305–1307. https://doi.org/10.1126/science.218.4579.1305.

Li G, Piper DJ, Campbell DC. 2011. The Quaternary Lancaster Sound trough-mouth fan, NW Baffin Bay. *Journal of Quaternary Science* **26**: 511–522. https://doi.org/10.1016/j.margeo.2017.09.002.

McGlannan AJ, Bart PJ, Chow JM, Anderson JB. 2017. On the influence of post-LGM ice shelf loss and grounding zone sedimentation on West Antarctic ice sheet stability. *Marine Geology* **392**: 151–169.

McMullen K, Domack EW, Leventer A, Lavoie C, Canals M. 2016. Grounding-zone wedges and mega-scale glacial lineations in the Mertz Trough, East Antarctica. *Geological Society, London, Memoirs* **46**: 241–242. https://doi.org/10.1144/M46.175.

Mosola AB, Anderson JB. 2006. Expansion and rapid retreat of the West Antarctic Ice Sheet in Eastern Ross Sea: possible consequence of over extended ice streams? *Quaternary Science Reviews* **25**: 2177–2196. https://doi.org/10.1016/j.quascirev.2005.12.013.

Nygård A, Sejrup HP, Haflidason H, Lekens WAH, Clark CD, Bigg GR. 2007. Extreme sediment and ice discharge from marine-based ice streams: New evidence from the North Sea. *Geology* **35**: 395–398. https://doi.org/10.1130/G23364A.1.

Ottesen D, Dowdeswell JA, Lanvik JY, Mienert J. 2007. Dynamics of the Late Weichselian ice sheet on Svalbard inferred from high-resolution sea-floor morphology. *Boreas* **36**: 286–306. https://doi.org/10.1111/j.1502-3885.2007.tb01251.x.

Ottesen D, Rise L, Knies J, Olsen L, Henriksen S. 2005. The Vestfjorden-Trænadjupet paleo-ice stream drainage system, mid-Norwegian continental shelf. *Marine Geology* **218**: 175–189. https://doi.org/10.1016/j.margeo.2005.03.001.

Ottesen D, Stokes CR, Rise L, Olsen L. 2008. Ice-sheet dynamics and ice streaming along the coastal parts of northern Norway. *Quaternary Science Reviews* **27**: 922–940. https://doi.org/10.1016/j.quascirev.2008.01.014.

Porter SC, Swanson TW. 1998. Advance and retreat rate of the Cordilleran Ice Sheet in southeastern Puget Sound region. *Quaternary Research* **50**: 205–213. https://doi.org/10.1006/qres.1998.2004.

Powell RD. 1991. Grounding-line systems as second order controls on fluctuations of temperate tidewater termini. In *Glacial Marine Sedimentation — Paleoclimatic Significance*, Ashley GM, Anderson JB

(eds). Geological Society of American Special Paper 261: Boulder; 75–94.

Powell RD, Alley RB. 1997. Grounding-line systems: processes, glaciological inferences and the stratigraphic record. In *Geology and Seismic Stratigraphy of the Antarctic Margin II*, Barker PF, Cooper AC (eds). American Geophysical Union Antarctic Research Series: Washington, DC; 169–187.

Powell RD, Domack EW. 1995. Modern glaciomarine environments. In *Glacial Environments: Volume 1. Modern Glacial Environments: Processes, Dynamics and Sediments*, Menzies J (ed). Butterworth-Heinmann: Oxford; 445–486.

Pritchard HD, Arthern RJ, Vaughan DG, Edwards LA. 2009. Extensive dynamic thinning on the margins of the Greenland and Antarctic ice sheets. *Nature* **461**: 971–975. https://doi.org/10.1038/nature08471.

Prothro LO, Simkins LM, Majewski W, Anderson JB. 2017. Glacial retreat patterns and processes determined from integrated sedimentology and geomorphology records. *Marine Geology* **395**: 104–119. https://doi.org/10.1016/j.margeo.2017.09.012.

Rignot E, Jacobs SS. 2002. Rapid bottom melting widespread near Antarctic ice sheet grounding lines. *Science* **296**: 2020–2023. https://doi.org/10.1126/science.1070942.

Sexton DJ, Dowdeswell JA, Solheim A, Elverhøi A. 1992. Seismic architecture and sedimentation in north-west Spitsbergen fjords. *Marine Geology* **103**: 53–68. https://doi.org/10.1016/0025-3227(92)90008-6.

Shepherd A, Wingham D. 2007. Recent sea-level contributions of the Antarctic and Greenland ice sheets. *Science* **315**: 1529–1532. https://doi.org/10.1126/science.1136776.

Shipp SS, Anderson JB, Domack EW. 1999. Seismic signature of the late Pleistocene fluctuation of the West Antarctic Ice Sheet system in Ross Sea: a new perspective, Part I. *Geological Society of America Bulletin* **111**: 1486–1516. https://doi.org/10.1130/0016-7606(1999)111<1486:LPHROT>2.3.CO;2.

Simkins LM, Anderson JB, Demet BP. 2017a. Grounding line processes of the southern Cordilleran Ice Sheet in the Puget Lowland. In *From the Puget Lowland to East of the Cascade Range: Geologic Excursions in the Pacific Northwest*, Haugerud RA, Kelsey HM (eds). Geological Society of America Field Guide 49: Boulder, CO; 53–65 https://doi.org/10.1130/2017.0049(03).

Simkins LM, Anderson JB, Greenwood SL. 2016. Glacial landform assemblage reveals complex retreat of grounded ice in the Ross Sea, Antarctica. In *Atlas of Submarine Glacial Landforms: Modern, Quaternary and Ancient*, Dowdeswell JA, Canals M, Jakobsson M, Todd BJ, Dowdeswell EK, Hogan KA (eds). Geological Society, London, Memoirs 46: London; 353–356.

Simkins LM, Anderson JB, Greenwood SL, Gonnermann H, Prothro LO, Halberstadt ARW, Stearns LA, Pollard D, DeConto RM. 2017b. Anatomy of a meltwater drainage system beneath the ancestral East Antarctic ice sheet. *Nature Geoscience* **10**: 691–697. https://doi.org/10.1038/NGEO3012.

Simkins LM, Greenwood SL, Anderson JB. 2018. Diagnosing ice sheet grounding line stability from landform morphology. *The Cryosphere* **12**: 2707–2726. https://doi.org/10.5194/tc-2018-44.

Simms AR, Milliken K, Anderson JB, Wellner JS. 2011. The marine record of deglaciation of the south Shetland islands, Antarctica since the last glacial maximum. *Quaternary Science Reviews* **30**: 1583–1601. https://doi.org/10.1016/j.quascirev.2011.03.018.

Stokes CR, Clark CD. 2002. Are long subglacial bedforms indicative of fast ice flow? *Boreas* **31**: 239–249. https://doi.org/10.1111/j.1502-3885.2002.tb01070.x.

Swanson TW, Caffee ML. 2001. Determination of ^{36}Cl production rates derived from the well-dated deglaciation surfaces of Whidbey and Fidalgo islands, Washington. *Quaternary Research* **56**: 366–382. https://doi.org/10.1006/qres.2001.2278.

Thorson RM. 1989. Glacio-isostatic response of the Puget Sound area, Washington. *Geological Society of America Bulletin* **101**: 1163–1174. https://doi.org/10.1130/0016-7606(1989)101<1163:GIROTP>2.3.CO;2.

Winsborrow MC, Andreassen K, Corner GD, Laberg JS. 2010. Deglaciation of a marine-based ice sheet: Late Weichselian palaeo-ice dynamics and retreat in the southern Barents Sea reconstructed from onshore and offshore glacial geomorphology. *Quaternary Science Reviews* **29**: 424–442. https://doi.org/10.1016/j.quascirev.2009.10.001.